Pergamon

0301-9322(94)00070-0

Int. J. Multiphase Flow Vol. 21, No. 2, pp. 193–206, 1995

0301-9322/95 $9.50 + 0.00

MEASUREMENT OF CIRCUMFERENTIAL AND AXIAL LIQUID FILM VELOCITIES IN HORIZONTAL ANNULAR FLOW

B. SUTHARSHAN[1], M. KAWAJI[1]† and A. OUSAKA[2]

[1]Department of Chemical Engineering and Applied Chemistry, University of Toronto, Toronto, Ontario, Canada MS5 1A4

[2]Department of Mechanical Engineering, Tokushima University, Tokushima, 770 Japan

(Received 28 April 1994; in revised form 2 October 1994)

Abstract—The mechanism of liquid transport around the inner perimeter of a tube in horizontal annular flow has been experimentally investigated by using a photochromic dye activation technique. The liquid film velocities in circumferential and axial directions were measured by forming a dark spot of dye trace in the liquid film in a non-intrusive manner and recording the subsequent motion of the spot trace with a high-speed video camera. The experiments were conducted in a 5.28 m long horizontal tube with 25.4 mm i.d. at near atmospheric pressure conditions using air and kerosene. Over the ranges of gas and liquid flow rates tested ($16 < J_G < 40$ m/s and $0.04 < J_L < 0.1$ m/s), the base film was always seen to drain down the tube wall. During the periodic passage of disturbance waves, however, the spot dye trace moved upward indicating the transport of liquid in an upward direction against the force of gravity. The ripples propagating upward over the base film were also observed to transport the liquid upward, however, their contributions were less significant compared to those of the disturbance waves. These results indicate that the liquid is transported to the upper part of the tube by the disturbance waves and not by the secondary gas flow or other mechanisms as previously hypothesized.

Key Words: annular flow, liquid film, photochromic dye activation, two-phase flow, disturbance wave, ripple, transport phenomena

1. INTRODUCTION

Annular flow of gas and liquid is often encountered in horizontal boiler tubes at high qualities. Liquid flows as a thin, continuous film attached to the inner wall of the tube, while the gas flows in the core region at high speeds. Although many investigations have been conducted on the flow structure of horizontal annular flow, the fundamental question of how the liquid is transported to the upper part of the tube to form a continuous film around the perimeter despite the downward force of gravity has not been fully resolved yet (Jayanti *et al.* 1990). Possible physical mechanisms of liquid transport that have been proposed over the years can be summarized as follows.

(a) Secondary gas flow mechanism first proposed by Pletcher & McManus (1965) and later modelled by Laurinat *et al.* (1985) and Lin *et al.* (1985). The liquid film is sustained on the tube wall by the upward transport of liquid near the gas–liquid interface due to secondary gas flow while the liquid near the wall would run down due to gravity.
(b) Liquid entrainment and deposition mechanism proposed first by Russell & Lamb (1965), and further investigated by Anderson & Russell (1970), Wilkes *et al.* (1980) and others. High amplitude waves break up at the interface due to the interfacial shear stress producing liquid droplets. Some of these droplets are transported towards the upper part of the tube in the form of a spray and deposited on the upper tube wall. When deposited, the droplets coalesce to form a thin liquid film which flows down the tube wall toward the bottom by the gravitational force.
(c) Wave spreading and mixing mechanism proposed by Butterworth & Pulling (1972). The coherence in disturbance wave is thought to be achieved by strong circumferential mixing

†To whom correspondence should be addressed.

within the liquid film and this mixing would have the effect of spreading or redistributing the liquid whenever a disturbance wave passes by.

(d) Pumping action due to a disturbance wave proposed by Fukano & Ousaka (1989). The disturbance waves carry the liquid towards the upper part of the tube by pumping action due to a pressure gradient along the decreasing height of the wave and the base film drains downward.

Although some of the above hypotheses were supported by various models' abilities to predict the circumferential distribution of the time-averaged liquid film thickness, there have been no definitive experimental data reported previously to validate any of the above-proposed mechanisms. For example, if the secondary flow of gas is significant to produce sufficiently large interfacial shear forces that can drag the liquid film upward against the force of gravity, the flow direction of the liquid film, if it can be observed, should mostly be upward and axial at least near the interface. On the other hand, if the disturbance waves are the main supplier of the liquid to the liquid film in the upper part of the tube, the liquid would be flowing upward during their passage but drain downward after the passage of each disturbance wave.

To answer the fundamental question on liquid transport mechanism in horizontal annular flow, some investigators have studied the time-dependent behaviour of the liquid film (Jayanti *et al.* 1990), but a direct measurement of the flow direction and velocity of liquid film in the circumferential direction is also needed to verify the proposed mechanisms. Such an investigation has been attempted by using a dye tracer technique by Anderson & Russell (1968) and Butterworth & Pulling (1972) among others. Recently, Hewitt *et al.* (1990) attempted to use a photochromic dye activation technique to measure the circumferential velocity in the liquid film, however, all of the above dye tracer experiments were unsuccessful in quantifying the circumferential motion of the liquid film in horizontal annular flow.

In the present work, the liquid film velocities in both circumferential and axial directions have been successfully measured using a photochromic dye activation technique in a novel manner, in order to determine unambiguously the liquid transport mechanism in an isothermal, fully-developed annular flow in a horizontal circular tube. Specifically, the flow direction and velocity of the liquid film around the circumference of the inner tube wall has been determined for the base film, disturbance waves and the base film with ripples propagating upward. A high-speed video camera was employed to capture the motion of the dye traces and the images recorded on video films were analysed digitally using an image analysis software to obtain quantitative data that are useful for validating the existing models of horizontal annular flow.

2. EXPERIMENTAL METHOD

A schematic diagram of the flow loop employed in this work is shown in figure 1. The working fluids were kerosene and air at room temperature and near atmospheric pressure. The flow loop consisted of liquid and air circulation systems, and a test section. From a 10-l. storage tank, kerosene was circulated through the test section by a centrifugal pump. The liquid flow rate was measured by a rotameter located between the pump and the test section. Compressed air from the building supply was passed through a pressure regulator, a rotameter and a flow control valve and injected into the flow channel through the inlet section. From the outlet of the test section, a mixture of liquid and gas flowed into a cyclone separator where the air was separated from the liquid and discharged into the atmosphere. The liquid was returned to the storage tank by gravity.

The test section consisted of a gas–liquid inlet section, test channel and cyclone separator. The test channel was a 5.28 m long, round tube with 25.4 mm i.d. and 33.4 mm o.d., and made of Pyrex glass which is transparent to ultraviolet light. The gas–liquid inlet section was made of a 127 mm i.d. glass pipe tapered to connect to the test channel. It provided sufficient space for mixing the gas and liquid and to minimize disturbances to the flow at the entrance.

The optical arrangement for measuring the instantaneous liquid film velocity using the photochromic dye activation technique is shown in figure 2. Pulses of ultraviolet light beam from a Lumonics excimer laser was fired at a rate of 50 or 100 Hz to activate the photochromic dye dissolved in the liquid. The dye used was TNSB, which readily dissolves in organic liquids. For

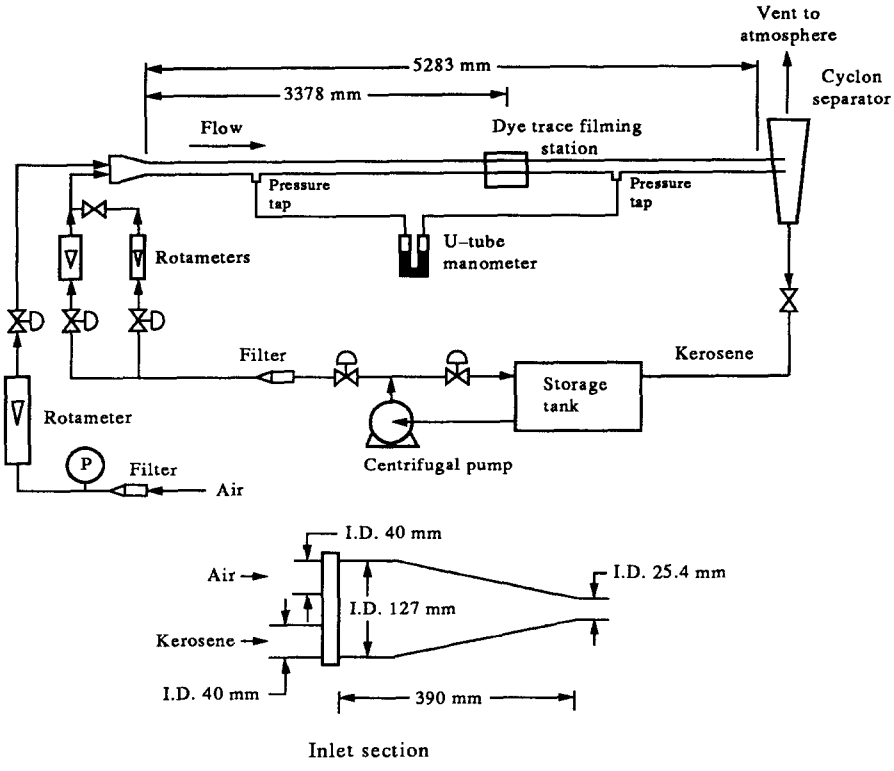

Figure 1. Schematic of two-phase flow loop and inlet section.

this work, the dye concentration of 0.06% by weight was used to achieve maximum contrast between the trace and the background. A neon–xenon–fluorine gas mixture was used to produce 351 nm wavelength u.v. light in the excimer laser. A u.v.-transmitting lens with a focal length of 130 mm was used to focus the beam on the inner wall of the test section. The lens was placed at a distance of about 180–200 mm away from the test section to form a small, circular spot trace in the thin liquid film, which could be easily identified and distinguished from the shades of ripples forming on the liquid film surface. The general aspects of the photochromic dye activation technique applied to two-phase flow have been recently given by Kawaji *et al.* (1993).

An optical correction box was also built around the flow channel and filled with dye-free kerosene to minimize optical distortion of the images in the tube when viewed from outside. The

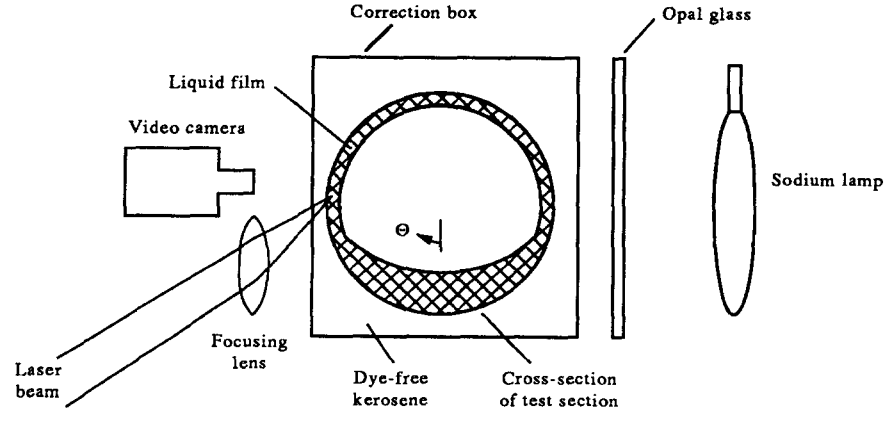

Figure 2. Optical arrangement for instantaneous velocity measurement.

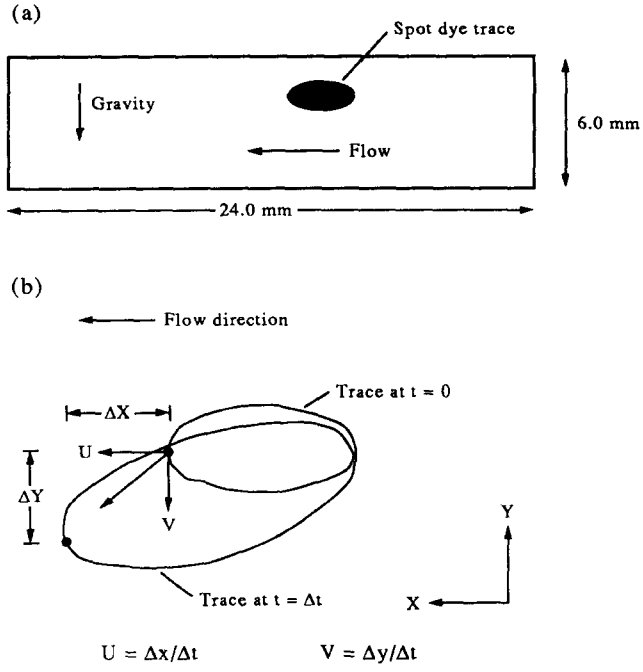

Figure 3. Observation of spot dye trace, (a) view frame and (b) determination of velocity components.

tube was surrounded by a correction box, made of Pyrex glass and filled with dye-free kerosene as shown in figure 2. The Pyrex glass has a refractive index of 1.47 compared with a value of 1.43 for kerosene, so that there is little distortion of the light ray passing through the correction box, test section and kerosene, all of which have virtually the same refractive index.

To record the displacement of the dye trace formed in the liquid, a high-speed video camera was utilized. This system had a CCD camera with 256 × 256 pixel resolution, varying frame speeds from 186 to 2066 frames per second (fps) depending on the size of the view field, and a shutter speed of up to 1/10,000 of a second. In this work, a rectangular view field of 24 mm in horizontal length and 6 mm in vertical height with a 256 × 64 pixel resolution was recorded at a rate of 744 fps and with a shutter speed of 1/1000 s^{-1}. The size of the view field and the initial location and shape of the spot dye trace are shown in figure 3(a).

The use of a high shutter speed necessitated adequate background lighting, which was provided by a 400 W sodium lamp powered by a 14 kHz AC power supply. This provided flicker-free background lighting for fast-video photography. A flash opal plate glass screen was also mounted between the correction box and the sodium lamp to diffuse the light for even illumination. Care was taken not to create dark shades of interfacial waves which can seriously interfere with the visualization of the dye trace.

3. TEST CONDITIONS AND IMAGE ANALYSIS

Five runs were performed in total and for each run the spot dye trace measurements were made at three different circumferential positions at angles of 45°, 90° and 135° from the bottom of the test channel. In every run, the following parameters were recorded: flow rates and temperatures of liquid and gas, frictional pressure drop and the absolute pressure reading at the first pressure tap. The experimental conditions are shown in table 1.

In the present tests, a continuous liquid film was observed to form around the inner tube wall in a length-to-diameter ratio, L/D, of less than 50 from the entrance in all cases. This left at least $L/D = 83$ for the annular flow to develop before the measurement location. In the horizontal annular flow experiments performed by Jayanti *et al.* (1990) using a 32 mm i.d. tube, the liquid

film thickness measured at $L/D = 110$ from the point of liquid injection through a porous wall was reported to have reached constant values at that location. Our entry length of $L/D > 83$ after the point of complete liquid film formation is not too different from Jayanti *et al.*'s value of $L/D = 110$. Also, in vertical annular flow, an L/D ratio of about 60 was sufficient for the liquid film thickness and pressure gradient to reach constant values after either porous injection or axial jet injection of liquid according to Gill *et al.* (1963) and Gill & Hewitt (1968). Thus, the annular flow in the present tests can be considered close to being fully developed at the measurement location.

The images of the spot dye traces recorded by the high-speed video camera were analysed using a PC-based digital image analysis system. The image analysing software, MOCHA, was used to analyse the motion of each spot dye trace in the following manner. The intensity of the background light (pixel intensity) was first adjusted to increase the contrast of the spot dye trace. Flood fill measurement was then used to define and measure the spot dye trace in the view field. First, an interior point was selected in the spot dye trace and MOCHA was used to distinguish the pixels which comprised the spot dye trace using a pixel criterion, color the spot dye trace to show its extent and make selected measurements in the colored region.

The measurements made on the spot dye trace were the major axis end points. The major axis was defined by searching all of the trace's border pixels and choosing the two pixels that are the farthest apart. It should be noted that the major axis was required to lie entirely within the boundary of the trace, starting and ending on boundary pixels. It was assumed that the maximum instantaneous velocity of the liquid phase is at the gas–liquid interface for a horizontal annular flow. Therefore, by choosing the major axis end points in the flood fill measurements, the interface velocity could be calculated as illustrated in figure 3(b). More details of the image analysis procedure can be found in Sutharshan (1993).

4. RESULTS AND DISCUSSION

The liquid film in horizontal annular flow consists of a thin base film, which flows with a smooth surface with some ripples, and disturbance waves which are thicker and rough on the surface, and propagate at much faster speeds than the ripples in the base film. The disturbance waves and the base film were easily distinguishable on the video tape by the shades of small ripples moving slowly on a smooth liquid surface for the base film and fast moving shades of rough interface observed for short intervals of time for the disturbance waves. When viewed in time sequence, the relatively longer periods of quiescent flow of the base film with little disturbance alternated with brief periods of rough disturbance waves passing by at much greater speeds.

Each disturbance wave did not, however, appear to be a single wave of large amplitude with a single peak. Instead, it was characterized by many rough waves of short wavelengths superimposed on a thick liquid film of finite length in the axial direction. Because of the limited width of the view field in the circumferential direction, it was not possible to determine the structure of the disturbance wave in the circumferenial direction such as the angle of inclination or curvature in the disturbance wave as suggested previously by Fukano & Ousaka (1989) and Jayanti *et al.* (1990).

4.1. Spot dye trace measurements

(A) Liquid transport in base film and disturbance waves. In contrast with an annular flow in a vertical tube where the liquid film thickness is uniform around the tube's inner perimeter, in horizontal annular flow more liquid flows near the bottom of the tube, the base film is thicker at the bottom and the film thickness decreases towards the top of the tube. The base film thickness

Table 1. Experimental conditions

Run No.	j_L (m/s)	j_G (m/s)
1	6.0×10^{-2}	16
2	6.0×10^{-2}	30
3	6.0×10^{-2}	40
4	4.0×10^{-2}	30
5	10.0×10^{-2}	30

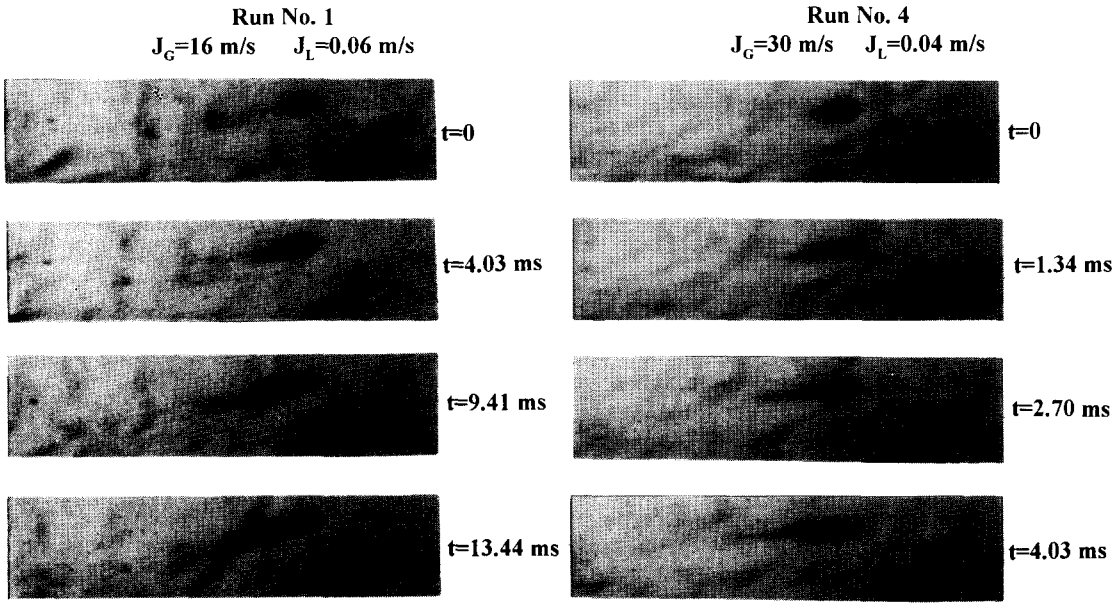

Figure 4. Motion of spot dye trace in base film (side measurement, $\Theta = 90$).

can, however, be assumed to be symmetrical with respect to the vertical plane which is drawn from the top to the bottom of the tube.

Two sequences of photographs in figure 4 show the movement of spot dye traces formed in the base film at the side of the tube ($\Theta = 90°$) in run 1 ($J_L = 0.06$ m/s, $J_G = 16$ m/s) and run 4 ($J_L = 0.04$ m/s, $J_G = 30$ m/s). Similar photographs for the other angular positions ($\Theta = 45°$ and 135°) and other runs can be found in Sutharshan (1993). The direction of flow was from right to left and the spot dye trace formed in the base film could be easily followed for more than ten consecutive frames (13 ms) in run 1, indicating absence of strong turbulent mixing or eddy motion in the base film. The movement of the spot dye trace in both runs indicated that the liquid in the base film drains downward at some angle from the horizontal, which is proportional to the *arctan* of the ratio of the circumferential to axial velocities. At the highest gas flow rate tested ($J_G = 40$ m/s), it was more difficult to observe the drainage of the base film from the original video tapes, but when the frames were magnified eight times with the aid of MOCHA, it was possible to determine the drainage angle in every run. As it may be observed by comparing the two sets of photographs shown in figure 4, the drainage angle decreased as the gas flow rate was increased, because of the increase in the axial velocity. It is also noted here that every dye trace observed indicated, without any exception, no upward motion of the liquid in the base film.

The motion of the spot dye trace in the disturbance waves is shown in figure 5 for runs 1 and 4. Again, the spot dye traces in these photographs were formed inside the disturbance wave at the side of the tube ($\Theta = 90°$). During the passage of each disturbance wave, the dye trace was seen to move upward, very rarely in purely the axial direction and never downward. Although the trace became dispersed much more quickly than in the base film, it remained visible long enough to determine the direction of liquid transport.

Since the amplitudes of the disturbance waves are much larger than the thickness of the base film, the trace formed in the disturbance wave may not represent the motion of the liquid near the interface. It is not certain how deep in the liquid layer the laser beam penetrated from the tube wall–liquid boundary, but the upward movement of the liquid observed even near the wall suggests that the entire liquid layer under the disturbance wave, and not just the region close to the interface, is involved in the upward transport of the liquid. It should also be noted here that the circumferential motion of the liquid under the disturbance wave could be directly observed in the present work for the first time, in contrast with the previous attempts including those by Butterworth & Pulling (1972) with dye injection flow visualization technique or Hewitt *et al.* (1990)

with a photochromic dye activation technique, which failed due to rapid dispersion of the dye in the disturbance wave.

The disturbance waves occupied more frames at smaller gas flow rates than at higher gas flow rates because their length in the axial direction decreased with the increasing gas flow rate. The frequency of the disturbance wave also increased as the gas flow rate was increased. These results are consistent with the measurements reported previously by Fukano *et al.* (1983) for air–water annular flow in a horizontal tube. In all cases, no two disturbance waves were exactly the same in axial length and the time interval between the passage of one disturbance wave and the arrival of the next was not always the same in any given run.

Based on the present video recordings of the dye trace movement, the instantaneous circumferential velocity data, V, are plotted against the axial velocity data, U, for the liquid film in figure 6 for three runs at two circumferential positions ($\Theta = 90^\circ$ and 135°). In these figures, the base film velocity and the disturbance wave liquid velocity are differentiated by using open and solid symbols, respectively. Negative circumferential velocities indicate downward flow from the top to the bottom of the tube.

The spot dye traces in the disturbance waves at $\Theta = 45^\circ$ could not be accurately analysed because the liquid film was thicker near the bottom of the tube and this made it difficult to distinguish the spot dye trace from various shades of the rough waves in the disturbance wave even by using the image analysis software. On the other hand, the spot dye trace at $\Theta = 90^\circ$ and 135° could be observed and tracked without much difficulty as shown in the photographs (figure 5). It is important to note here that the velocity data for the disturbance waves represent the velocity of the liquid in the disturbance wave and not the wave velocity. Also, because of the large amplitude of the disturbance waves and finite depth of penetration of the laser beam in the liquid film, the velocities obtained could be somewhat less than the actual velocities of the gas–liquid interface.

As it can be seen in figure 6, the base film liquid always has a velocity component in the downward direction toward the bottom of the tube, while the liquid in the disturbance wave has an upward velocity toward the top of the tube, in addition to the axial velocity component. The axial velocity of the base film increased with the increasing gas flow rate. The liquid in the disturbance wave also moved faster in the axial direction at higher gas and liquid flow rates. However, the circumferential velocity components of the base film and the disturbance wave liquid were widely distributed and it was difficult to discern any pattern. Nonetheless, certain differences can be noted by comparing the velocity components of the base film or the disturbance wave at different positions on the circumference. The downward velocities of the base film at $\Theta = 90^\circ$ are

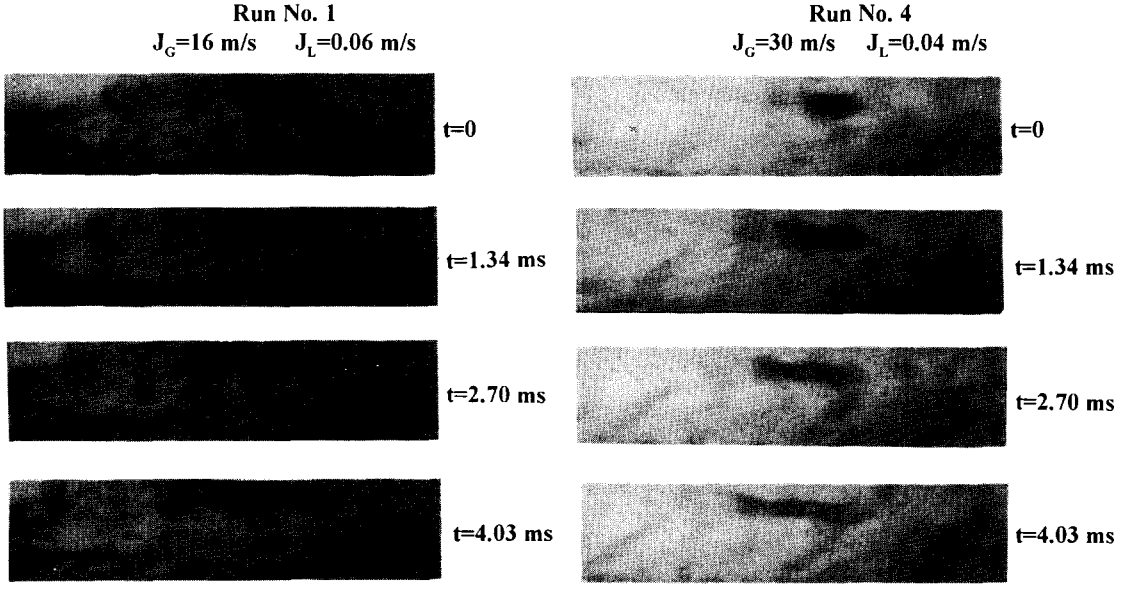

Figure 5. Motion of spot dye trace in disturbance wave (side measurement, $\Theta = 90^\circ$).

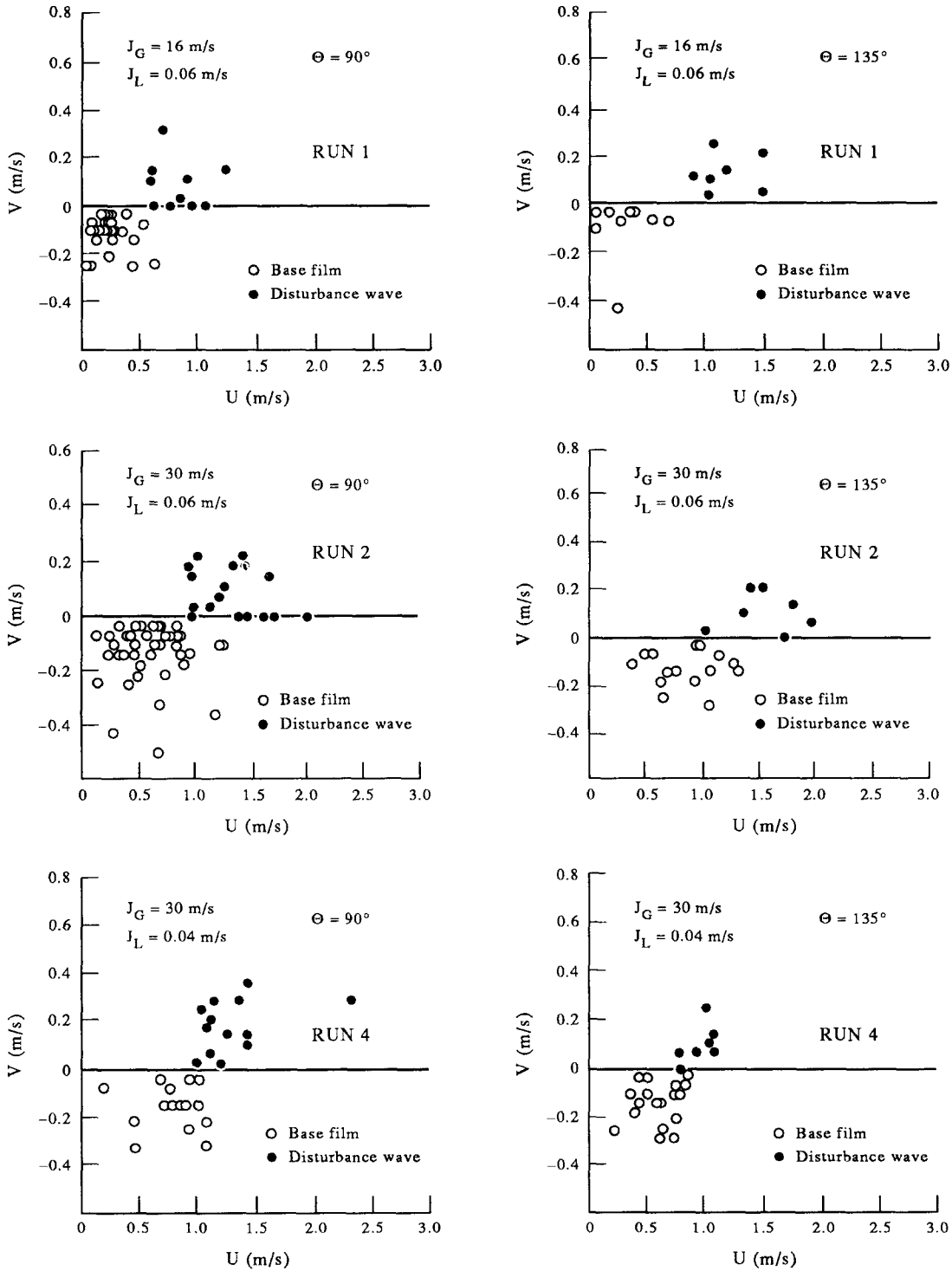

Figure 6. Axial and circumferential velocity components in base film and disturbance waves.

seen to be generally greater than those at $\Theta = 135^\circ$ due to the effect of gravitational acceleration downward. On the other hand, greater upward velocities are observed for the liquid in the disturbance wave at $\Theta = 90^\circ$ than at $\Theta = 135^\circ$. This is again due to the force of gravity decelerating the upward motion of the liquid in the disturbance wave. At all circumferential positions, the axial velocity of the base film was observed to be higher just behind the disturbance wave and to decrease

continuously until the next disturbance wave came. This means that the drainage angle would vary with time after the passage of each disturbance wave.

It is clear from the present data that the disturbance waves supply the liquid to the top of the tube and replenish the base film, and between the passage of two consecutive disturbance waves the liquid in the base film drains continuously due to gravity. Therefore, the disturbance wave plays the most important role in supplying the liquid to the upper wall of the tube within the present range of test conditions.

(B) Liquid transport by ripples or small waves. The ripples or small waves also appeared on the base film during the period between the passage of disturbance waves. Unlike the disturbance waves, however, the width and amplitude of the ripples were very small. At the lowest gas flow rate tested, $J_G = 16$ m/s, the number of ripples observed was less compared to that at higher gas flow rates. Furthermore, a larger number of ripples were observed just before and after the passage of the disturbance wave and the direction of motion of the ripples changed with time as illustrated in figure 7. Just after the passage of a disturbance wave, ripples were observed to travel upward from the bottom to the top of the tube. After a little while, the ripples propagated in the axial direction, then downward. Just before the arrival of the next disturbance wave, the ripples again travelled upward towards the top of the tube.

The motion of the spot dye trace formed in the base film was seen to be affected by the ripples travelling axially and upward at a speed faster than that of the dye trace. Figure 8 shows the effect of a ripple on the motion of the dye trace in the base film in run 1 at the side of the tube, $\Theta = 90°$. The leading edge of the spot dye trace is seen to first move downward, then horizontally and finally upward when the ripple, which was propagating in the upward direction, passed over the dye trace. This upward transport of liquid by the ripples was seen, however, only for short periods just after the passage or before the arrival of a disturbance wave.

Figure 9 shows a plot of the instantaneous circumferential velocity, V, against the instantaneous axial velocity, U, for the base film when ripples were propagating upward over the dye trace. The circumferential velocities were in all cases positive indicating upward transport of liquid in the base film. The average circumferential velocities, obtained by averaging the data shown in figure 9, increased with the gas and liquid flow rates as shown in figure 10. Also shown are the magnitudes of the average circumferential velocities for the base film without any ripples obtained from the instantaneous velocity data shown in figure 6. Although the directions of circumferential velocity were opposite with and without the ripples propagating upward, the trend was the same. The magnitudes of the average circumferential velocities were, however, slightly smaller for the liquid film with the upward propagating waves than those without. This means that even if the base film were covered by the upward propagating ripples half of the time, the time-averaged velocity of the

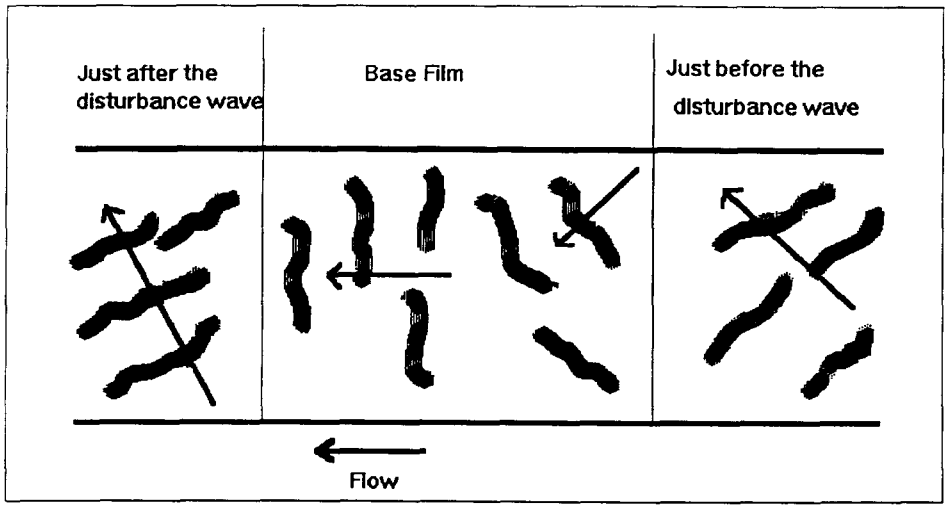

Figure 7. Motion of ripples propagating over base film.

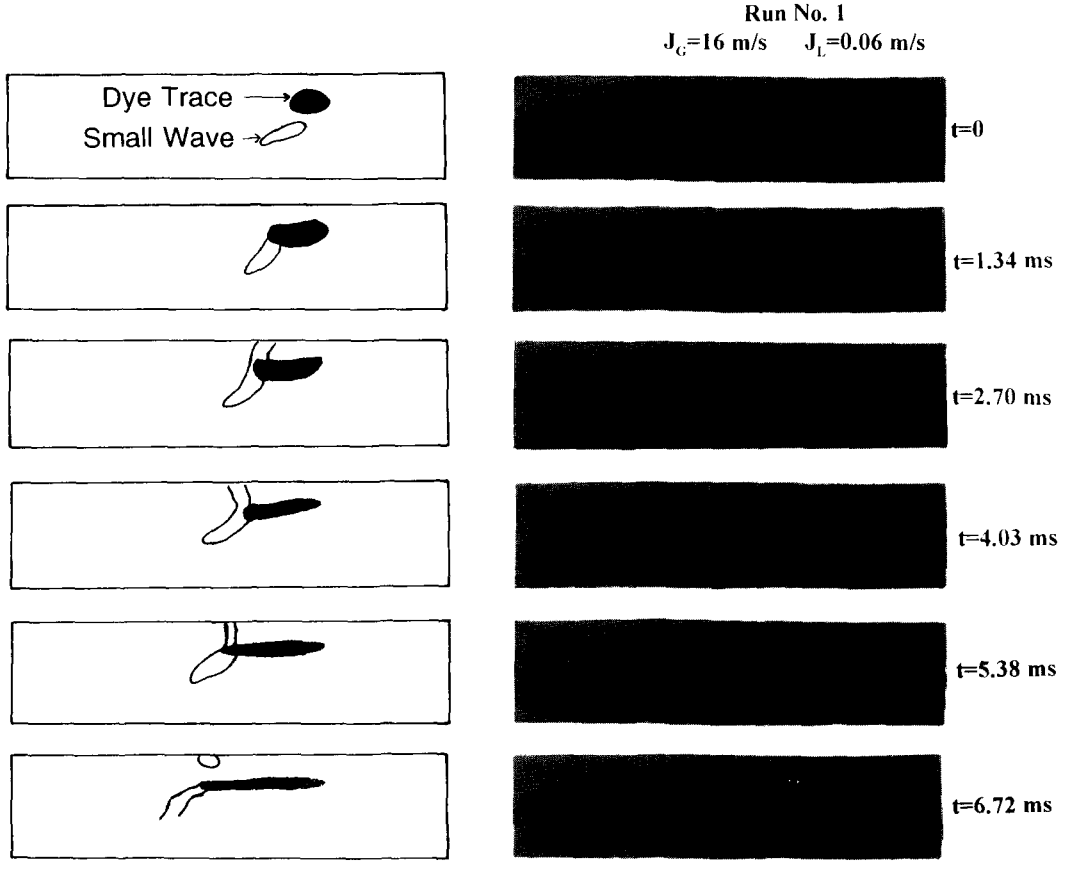

Figure 8. Motion of spot dye trace in base film during passage of an upward-moving ripple (run 1, side measurement).

base film would still be negative and the liquid would drain downward. At the liquid and gas flow rates tested, the wavelengths and frequency of passage were too low for the upward propagating ripples to contribute significantly to the overall upward transport of liquid in the liquid film. Their importance may, however, increase at lower liquid and higher gas flow rates, when the frequency of disturbance waves is significantly diminished and the base film is covered only by the ripples.

4.2. Comparison with time-dependent film thickness data

The continuous drainage of the base film due to gravity after the passage of a disturbance wave as observed in the photochromic dye trace measurements is also consistent with the time-dependent, local liquid film thickness data reported by Jayanti *et al.* (1990). They measured the temporal variations in the local liquid film thickness using electrical conductance probes in air–water annular flow in a horizontal tube of 32 mm i.d. The superficial gas and liquid velocities used were similar to those in the present work and the time-dependent variations in the film thickness were measured at the top, side and bottom of the tube.

Their data showed frequent appearance of sharp peaks in the film thickness corresponding to the passage of large-amplitude disturbance waves and gradual decrease in the liquid film thickness at the top and side after the passage of each disturbance wave. Those results can be explained by the observations of the motion of the spot dye traces discussed earlier. In addition, the small amplitude fluctuations in the film thickness data observed between the sharp peaks corresponding to the disturbance waves, are likely associated with the surface ripples or the small waves propagating over the base film.

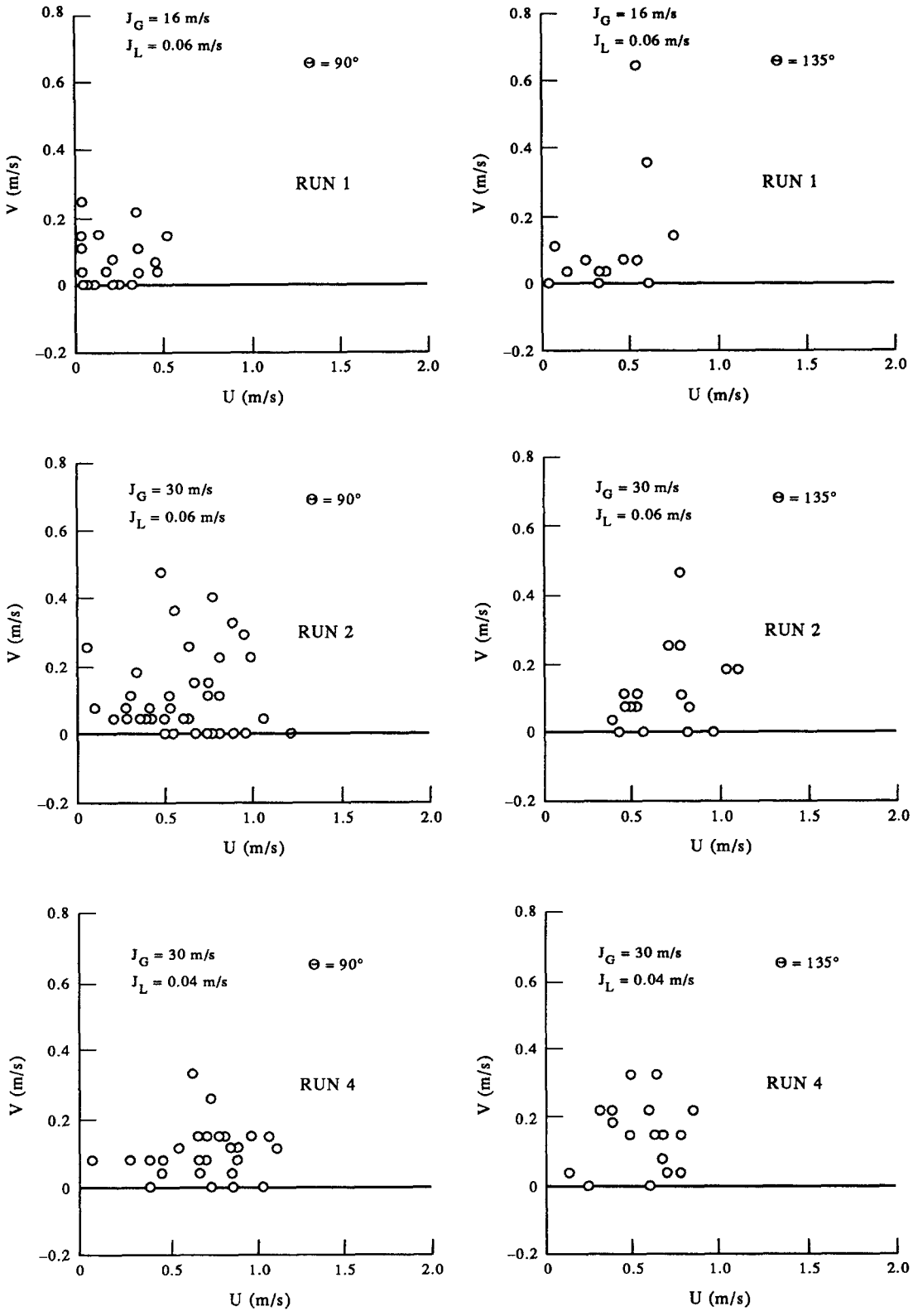

Figure 9. Axial and circumferential velocity components under upward-moving ripples.

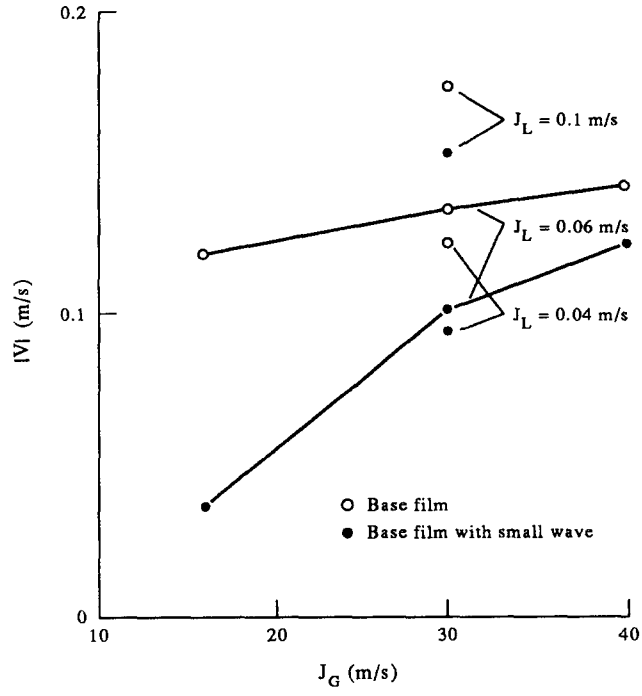

Figure 10. Variation of average circumferential velocity with superficial gas velocity (side measurement, $\Theta = 90°$).

5. LIQUID TRANSPORT MECHANISM IN HORIZONTAL ANNULAR FLOW

In this section the four important mechanisms, which have been previously proposed for liquid transport in horizontal annular flow, are reconsidered and their validity discussed in view of the results obtained in the present work.

5.1. Secondary gas flow mechanism

It is assumed that the secondary gas flow occurs in horizontal annular flow as a result of an axially asymmetric liquid film thickness distribution and varying interfacial roughness in the circumferential direction. This secondary gas flow is thought to induce sufficiently large shear forces at the gas–liquid interface which cause the liquid near the interface to continuously move upward, while the liquid near the wall would run down due to gravity. If the liquid near the gas–liquid interface is indeed carried upward by interfacial shear, the spot dye trace formed near the interface would have always moved upward. However, no part of the spot dye trace was seen to move upward in the base film except when the disturbance waves or ripples passed by. Therefore, it can be definitively concluded that the secondary flow of gas does not play a direct role in the upward transport of liquid at superficial gas velocities up to 40 m/s.

5.2. Wave mixing and spreading

According to this model the disturbance waves in horizontal annular flow are thought to be coherent around the perimeter and this coherence is achieved by strong circumferential mixing within the liquid film. This mixing would have the effect of spreading or redistributing the film whenever a disturbance wave passes by. It was observed in the present work that the spot dye trace moved only in the upward direction and never downward in the disturbance wave, which does not support the idea of strong mixing. Therefore, although it is obvious from the data that the disturbance waves supply the liquid to the upper part of the tube, the mechanism by which the disturbance wave spreads the liquid is not by strong mixing. Although the ripples or small waves were also observed to transport the liquid upward whenever those waves were propagating upward just before and after the passage of a disturbance wave, the action of the ripples alone is not

sufficient to maintain a liquid film in the upper part of the tube. Its importance in redistributing the liquid film is negligible compared to the disturbance waves when the liquid and gas flow rates are within the ranges of the present study. The role of the ripples may become more significant at higher gas and lower liquid flow rates when the frequency of their appearance increases while the disturbance waves occur less frequently.

5.3. Entrainment and deposition of liquid droplets

In the video pictures of the base liquid film, no significant droplet deposition on the liquid film was observed in the upper part of the tube. For the case of the lowest gas flow rate ($J_G = 16$ m/s), there were practically no signs of droplet deposition on the liquid film. The onset of liquid entrainment in horizontal annular flow has been determined to depend on both liquid and gas flow rates, and for $J_L = 0.06$ m/s in air–water systems it has been reported to occur at $J_G = 15$ m/s (Ousaka & Kariyasaki 1992). Although the onset of entrainment in air–kerosene annular flow may occur at a somewhat different gas velocity, liquid entrainment and deposition phenomena were unlikely responsible for supplying the liquid to the upper part of the tube at the lowest gas flow rate ($J_G = 16$ m/s) tested in this work. At $J_G = 30$ and 40 m/s, some instances of droplet deposition were observed, however, the deposition rate was observed to be much too low to account for the transport of liquid and replenishing of the liquid film in the upper part of the tube. In longer tubes, the flow rate of entrained liquid would be greater and the entrainment/deposition mechanism could play a more significant role. Nevertheless, the present results indicate that a continuous liquid film can be formed and maintained on the entire inner perimeter of the tube without the entrainment/deposition mechanism.

5.4. Pumping action of disturbance waves

As Fukano & Ousaka (1989) proposed, it has become quite clear from this experimental work that in horizontal annular flow, the disturbance wave is the most important factor in supplying the liquid to the upper part of the tube wall and maintaining a liquid film against the force of gravity. Furthermore, in between the passage of disturbance waves, the liquid film drains continuously downward due to gravity. However, the exact physical mechanism by which the disturbance waves transport the liquid upward needs to be further clarified in the future.

Finally, it should be noted that the present results have important practical implications for prevention of liquid film dryout in horizontal boiler tubes in which annular flow is often encountered at high qualities. Since the inner surface of the boiler tube is continuously wetted by a liquid film maintained mainly by the action of the disturbance waves, further research into the nature of these waves and means to increase the frequency of their occurrence will be highly useful for prevention of liquid film dryout in the boiler tubes. Of course, under sufficiently high gas flow rates and in longer tubes, liquid entrainment and deposition phenomena would increase in importance and thus, the relationship between the disturbance waves and entrainment/deposition phenomena also needs further investigation.

6. CONCLUSIONS

The photochromic dye activation technique has been successfully used in the study of horizontal annular flow to measure the instantaneous velocities of a liquid film in both circumferential and axial directions at several positions around the inner perimeter of a tube. The results obtained in this work have clearly shown that under the present test conditions the disturbance waves play the most important role in transporting the liquid to the upper part of the horizontal tube against the force of gravity, which confirms the basic assumption of Fukano & Ousaka's (1989) model. During the period between the passage of disturbance waves, the liquid in the base film was found to continuously drain downward due to gravity.

These results clearly show that the secondary flow in the gas core proposed previously to be the major contributor to the upward liquid transport is not valid. The small amplitude ripples on the base film were also seen to carry the liquid upward, whenever the ripples were propagating upward, but their contribution to the overall upward transport of liquid was determined to be quite small compared to that of the disturbance waves, especially at low liquid and gas flow rates. The present

results are consistent with the time-dependent variations in local film thickness reported by Jayanti *et al.* (1990) for air–water annular flow in a horizontal tube at similar gas and liquid flow rates.

Acknowledgements—This work was financially supported by the Natural Sciences and Engineering Research Council of Canada and A. Ousaka's research leave was assisted by funding from the Japan Atomic Energy Research Institute.

REFERENCES

ANDERSON, R. J. & RUSSELL, T. W. F. 1970 Film formation in two-phase annular flow. *AIChE Jl* **16,** 626–633.

BUTTERWORTH, D. & PULLING, D. J. 1972 A visual study of mechanisms in horizontal annular air-water flow. UKAEA Report No. AERE-M2556.

FUKANO, T. & OUSAKA, A. 1989 Prediction of the circumferential distribution of film thickness in horizontal and near horizontal gas–liquid annular flow. *Int. J. Multiphase Flow* **15,** 403–419.

FUKANO, T., OUSAKA, A., MORIMOTO, T. & SEKOGUCHI, K. 1983 Air–water annular flow in a horizontal tube (Part II: circumferential variation of film thickness parameters). *Bull. JSME* **26,** 1387–1395.

GILL, L. E. & HEWITT, G. F. 1968 Sampling probe studies of the gas core in annular two-phase flow—III. Distribution of droplet flow rate after injection through an axial jet. *Chem. Engng Sci.* **23,** 677–686.

GILL, L. E., HEWITT, G. F., HITCHON, J. W. & LACEY, P. M. C. 1963 Sampling probe studies of the gas core in annular two-phase flow—I. The effect of length on phase and velocity distribution. *Chem. Engng Sci.* **18,** 525–535.

HEWITT, G. F., JAYANTI, S. & HOPE, C. B. 1990 Structure of thin liquid films in gas–liquid horizontal flow. *Int. J. Multiphase Flow* **16,** 951–957.

JAYANTI, S., HEWITT, G. F. & WHITE, S. P. 1990. Time-dependent behaviour of the liquid film in horizontal annular flow. *Int. J. Multiphase Flow* **16,** 1097–1116.

KAWAJI, M., AHMAD, W., DEJESUS, J. M., SUTHARSHAN, B., LORENCEZ, C. M. & OJHA, M. 1993 Flow visualization of two-phase flows using photochromic dye activation method. *Nucl. Engng Design* **141,** 343–355.

LAURINAT, J. E., HANRATTY, T. J. & JEPSON, W. P. 1985 Film thickness distribution for gas–liquid annular flow in a horizontal pipe. *PhysicoChem. Hydrodynam.* **6,** 179–195.

LIN, T. F., JONES, O. C., LAHEY, R. T., BLOCK, R. C. & MURASE, M. 1985 Film thickness measurements and modelling in horizontal annular flows. *PhysicoChem. Hydrodynam.* **6,** 197–206.

OUSAKA, A. & KARIYASAKI, A. 1992 Distribution of entrainment flow rate for air–water annular two-phase flow in a horizontal tube. *JSME Int. J. (Ser. 2)* **35,** 354–360.

PLETCHER, R. H. & MCMANUS, H. N. 1965 The fluid dynamics of 3-dimensional liquid films with free surface shear: a finite difference approach. In *Proc. 9th Midwestern Mechanics Conf.*, Madison, WI.

RUSSELL, T. W. F. & LAMB, D. E. 1965 Flow mechanism of two-phase annular flow. *Can. J. Chem. Engng* **43,** 237–245.

SUTHARSHAN, B. 1993 Investigation of liquid transport mechanisms in horizontal annular flow. M.A.Sc. thesis, Department of Chemical Engineering and Applied Chemistry, University of Toronto.

WILKES, N. S., CONKIE, W. & JAMES, P. W. 1980 A model for the droplet deposition rate in horizontal two-phase annular flow. UKAEA Report No. AERE-R9691.